

Mean Field Calculations of the Dynamic Mechanical Properties of Two-Phase Elastomer Blends: Included Particles in a Matrix Phase

K. A. MAZICH, H. K. PLUMMER, JR., M. A. SAMUS, and
P. C. KILLGOAR, JR., *Research Staff, Ford Motor Company,
Dearborn, Michigan 48121-2053*

Synopsis

Mean field theories developed by Kerner and van der Poel were applied to several binary elastomer blends. Calculations were compared with experimental small strain dynamic mechanical properties of the blends. Although the blends exhibit a wide range of detailed structures, the theories were able to model blends with well-defined included particles embedded in a matrix phase. Blends with a continuous morphology were not properly modeled with the Kerner or van der Poel theories.

INTRODUCTION

Our work is focused on the application of several blending laws that predict the small strain dynamic mechanical properties of elastomer blends from the measured properties of the pure components in the blend. Two theories that employ mean field arguments were used to calculate dynamic mechanical properties of the elastomer blends. One equation was developed by Kerner¹ and another proposed by van der Poel² and corrected by Smith.^{3,4} Both theories calculate a mechanical response for an average spherical particle surrounded by a shell of matrix material. This average composite particle is embedded in a medium of material with the (unknown) bulk properties of the composite. The mechanical properties of this average particle represent the average mechanical response of the bulk composite. Particle interactions are not considered in this model. In this sense, there should be some limiting concentration of particles for the appropriate application of the theory.

Previous calculations using the Kerner and van der Poel equations have been applied successfully to two types of heterogeneous polymer composites.⁵⁻⁷ These are particulate-filled rubbers and rubber-modified thermoplastics. They are characterized by the widely separate glass transition temperatures of the components in the blend. The work reported in this article has been performed on elastomer blends. In these systems, the glass transition temperatures of the components are not necessarily widely separated from one another. In this work, we compared the predictions of the Kerner and van der Poel/Smith equations to the measured temperature dependence of the small

strain dynamic mechanical properties. We varied the composition of the blends and tested the accuracy of the theoretical predictions for the various blend structures that were generated. In addition, we examined the structure of the elastomer blends with transmission electron microscopy to determine the types of morphology that are successfully modeled by the calculations.

THEORY

For a heterogeneous binary composite containing suspensions of one component in a matrix of the second component, Kerner's¹ result for the shear modulus (G) is

$$\frac{G^*}{G_m^*} = \frac{(1 - \phi_i)G_m^* + (\alpha + \phi_i)G_i^*}{(1 + \alpha\phi_i)G_m^* + \alpha(1 - \phi_i)G_i^*} \quad (1)$$

In this expression, G^* is the dynamic (complex) shear modulus of the composite, ϕ_i is the volume fraction of inclusions, subscript i designates a property of the suspensions, m designates a property of the matrix, and superscript $*$ designates a complex quantity. In Eq. (1), $\alpha = (8 - 10\mu_m^*) / (7 - 5\mu_m^*)$, where μ_m^* is Poisson's ratio for the matrix. Substituting Eq. (2)

$$E^* = 2G^*(1 + \mu^*) \quad (2)$$

into Eq. (1), casts Kerner's equation in terms of the tensile modulus, E^* . To simplify the calculation, we follow the assumption that μ^* is real, that is, $\mu^* = \mu$.⁸ In addition, we need to estimate the temperature dependence of μ_m to calculate the temperature dependence of the composite tensile modulus, E^* . For this purpose, we chose a functional form that corresponds to the temperature dependence of the storage modulus of the matrix material, E'_m . The expression

$$\mu_m(T) = .17 \left[\frac{\log E'(\text{glass}) - \log E'(T)}{\log E'(\text{glass}) - \log E'(\text{rubber})} \right] + .32 \quad (3)$$

allows μ_m to vary from .32 in the glassy region to .5 in the rubbery region. In Eq. (3), $\log E'(\text{glass})$ is the value of $\log E'$ in the glassy region, $\log E'(\text{rubber})$ is the value of $\log E'$ in the rubbery region, and $\log E'(T)$ is the value of $\log E'$ at the temperature of interest. Trial calculations with other values for μ_m did not alter the results substantially, indicating that Kerner's theory for dispersions is not very sensitive to the value of μ_m .

Smith's correction^{3,4} of van der Poel's derivation² of the mechanical properties of heterogeneous composite media yields the quadratic equation

$$\alpha X^2 + \beta X + \tau = 0 \quad (4)$$

where

$$\alpha = [4P(7 - 10\mu_m) - Sa^7][Q - (8 - 10\mu_m)(M - 1)\alpha^3] - 126P(M - 1)\alpha^3(1 - \alpha^2)^2$$

$$\beta = 35(1 - \mu_m)P[Q - (8 - 10\mu_m)(M - 1)\alpha^3] - 15(1 - \mu_m)[4P(7 - 10\mu_m) - Sa^7](M - 1)\alpha^3$$

$$\tau = -525P(1 - \mu_m)^2(M - 1)\alpha^3$$

$$P = M(7 + 5\mu_i) + 4(7 - 10\mu_i)$$

$$Q = M(8 - 10\mu_m) + (7 - 5\mu_m)$$

$$S = 35M(7 + 5\mu_i)(1 - \mu_m) - P(7 + 5\mu_m)$$

$$M = G_i^*/G_m^*$$

$$X = (G^*/G_m^* - 1)$$

$$\alpha^3 = \phi_i$$

We calculated the coefficients of the quadratic Eq. (4) with pure component values for μ_i , μ_m , G_i^* , and G_m^* . Assumptions regarding the temperature dependence of μ_i and μ_m were identical to those given above for Kerner's dispersion model. The solution of Eq. (4) yields the calculated value for the complex modulus of the composite through the definition of X .

EXPERIMENTAL

Binary blends studied in this work consisted of natural rubber (NR) (SMR-L, MRPRA) mixed with either bromobutyl rubber (BIIR) (Bromobutyl X2, Polysar Ltd.) or polyisobutylene (IM) (Vistanex L-140, Exxon Chemical Co.). The polymers were banded and mixed at room temperature on a small two-roll mill and allowed to relax for 24 h before the curatives were added. The cure temperature was 150°C and an oscillating disk rheometer was used to determine the cure time. A specimen of polyisobutylene was prepared by pressing the material at 100°C into a slab approximately 2 mm thick. All compounds contained Agerite Resin D (1 phr), Sulfur (1 phr), Methyl Tuads (1 phr), ZnO (5 phr), and Stearic Acid (1 phr). The polymer ratio varied from 75(phr)/25(phr) to 25/75 for the various blends.

The dynamic mechanical properties of the blends and the pure polymers were measured on a Polymer Laboratories Dynamic Mechanical Thermal Analyzer in the dual cantilever mode. Materials were subjected to oscillating deformations at 10 Hz while the temperature was increase at 2°C/min. The amplitude of the deformation was $\sim 65 \mu\text{m}$.

Samples of the binary blends were prepared for observation and analysis in the transmission electron microscope (TEM) using an LKB Ultratome III

cryomicrotome. Some samples were coated with a layer of evaporated carbon for conductivity after microtoming. Additional thin sections of each sample (samples that were not subjected to prior TEM analysis) were suspended over a solution of 1% osmium tetroxide in a closed container for 16 h to add a heavy metal stain to sites of unsaturation in the polymers. A Siemens Elmiskop 102 TEM (125 kV) and a JEOL 2000 FX Analytical Electron Microscope (AEM) (200 kV) were used to determine polymer morphology. A high-angle energy-dispersive X-ray detector on the JEOL AEM provided elemental composition of individual regions of the samples.

RESULTS AND DISCUSSION

A series of NR/BIIR blends and NR/IM blends were prepared to study the ability of the Kerner and van der Poel/Smith equations to correctly calculate the dynamic mechanical properties of elastomer blends. The compositions of these blends were varied to change the structure of the blends from particulate-filled matrices to continuous, interconnected morphologies. Theoretical calculations were compared with data for the various structures to outline the type of blend structure that corresponds to correct model predictions.

Natural rubber was the common component in all of the blends studied. BIIR or IM was chosen as the second component to study the effect of long-range molecular architecture on the mechanical properties of the blend. BIIR and IM contain isobutylene as the monomeric unit. And the mechanical properties of blends with either of these components should be very similar for relatively short-range rearrangements in the molecular structure (through the glass transition). In contrast, the long-range rearrangements available to the blend may vary for composites containing IM and BIIR. The sites of unsaturation pendant to the macromolecular backbone in BIIR (approximately one site for every 100 carbon atoms along the backbone) may allow crosslinking within the BIIR phase and with neighboring NR molecules at the phase interface. Unsaturation is found in IM only at one terminal site. Thus, IM cannot form a covalently linked network structure. These differences, in conjunction with differences in molecular weight between BIIR and IM, could account for varied mechanical behavior in experiments that probe the long range structure of the elastomer blend (frequencies and temperatures corresponding to properties well into the rubbery region).

The experimental results reported here encompass the glass transition region of the component polymers in the elastomer blend. The dual cantilever geometry used to measure dynamic mechanical data does not allow accurate measurement of properties well into the rubbery region. For this reason, the program described here will test mean field theories for shorter range mechanisms only (molecular rearrangements that account for the glass transition). In this regard, we expect that the results for NR/IM and NR/BIIR blends will be very similar.

Experimental values of the storage modulus, E' , and the loss tangent, $\tan \delta$, are shown in Figure 1 for a 75/25 blend of NR and IM. From experimental data on each pure component [presented in Fig. 2 and discussed in reference (9)], we identify the peak in the loss tangent at -45°C and 10 Hz with the

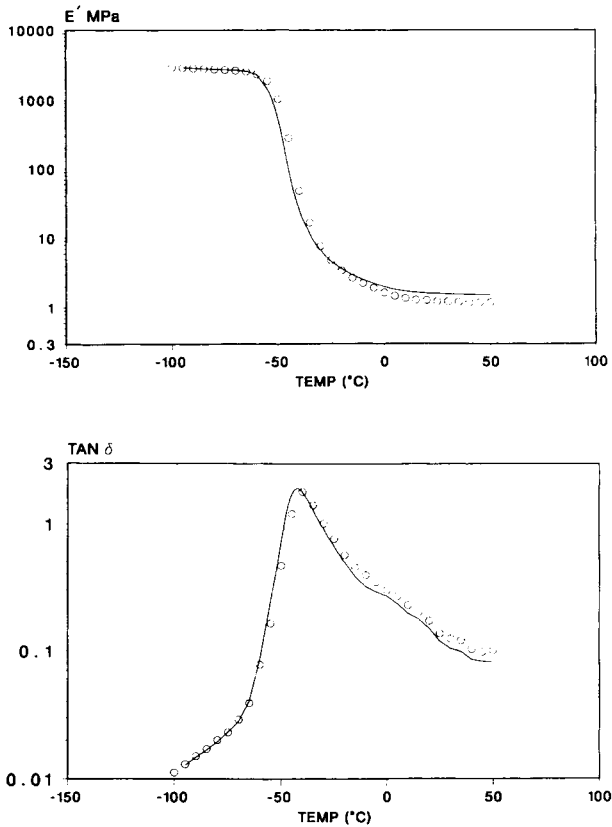


Fig. 1. Storage modulus and loss tangent vs. temperature for the NR/IM, 75/25 blend. Kerner and van der Poel calculations are represented by the solid line.

glass transition of NR and the broad shoulder around 0°C and 10 Hz with the glass transition of IM. The breadth of the experimental temperature region presented in the figure largely corresponds to the transition regions for the components in the elastomer blend. Results for a 75/25 blend of NR and BIIR (not shown) were very similar to the results for the 75/25 blend of NR and IM, as discussed above.

Calculations were performed for the elastomer blends by choosing the component that forms the included phase and choosing the volume fraction of inclusions in the blend. Further assumptions regarding the structure of the blend can be made by deciding the type of inclusion that is present in the blend. Inclusions can be isotropic and homogeneous, containing only one component of the blend. Alternatively, inclusions may be two-phase structures themselves, containing inclusions within inclusions. The assumptions that are used to perform the calculations suggest various structures that the blend can exhibit. Theoretical results based on these various structures were compared with data to indicate a likely structure for the blend.

Kerner and van der Poel/Smith calculations were performed for the 75/25 blends of NR/IM and NR/BIIR assuming that the minor component (IM or BIIR) is the included phase and the volume fraction of inclusions is equal to

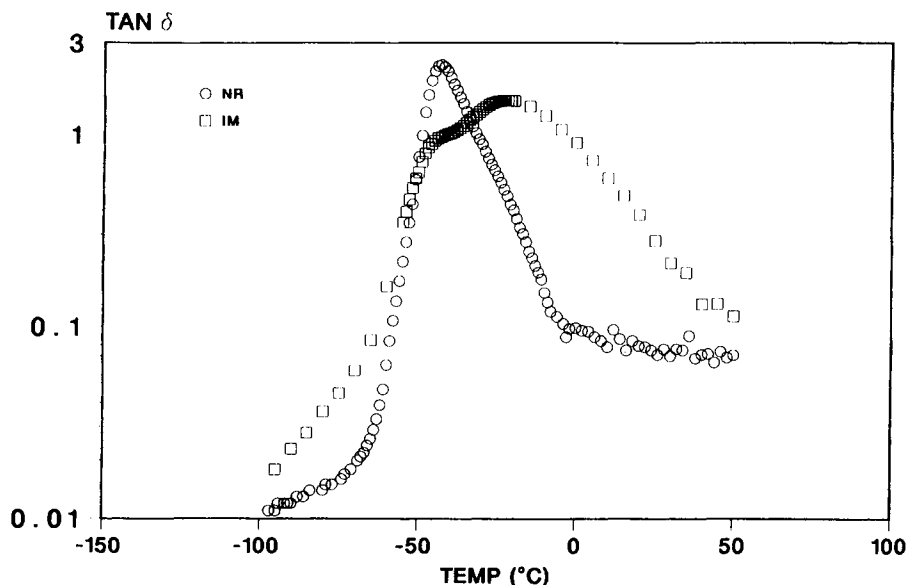


Fig. 2. Loss tangent vs. temperature for pure component NR (○) and pure component IM (□).

the weight fraction of the minor component used to prepare the blend ($\phi_2 = 0.25$). We also assumed that the inclusions were isotropic and homogeneous. The calculations are shown as the solid curve in Figure 1. (Similar results were generated for the 75/25, NR/BIIR blend.) The good agreement between the theoretical calculations and the experimental data verify the ability of mean field theories to model dynamic mechanical data of elastomer blends in the range of temperature (and frequency) depicted in Figure 1. The agreement also implies that well-defined, homogeneous inclusions of IM or BIIR are embedded in a NR matrix.

Transmission electron microscopy (TEM) was used to study the structures of the blends presented above and to verify or refute the conclusions drawn from mechanical analysis. A micrograph of a stained thin section of NR/IM (75/25) is shown in Figure 3. The light, roughly spherical included phase, is polyisobutylene. The inclusions range from 200 nm to several microns in size. Micrographs of the 75/25 NR/BIIR blend (not shown) also exhibit approximately spherical inclusions of BIIR in a NR matrix. The inclusions are smaller than the NR/IM blend (averaging 0.5 μm). And the boundary between the NR phase and BIIR phase appears more distinct than the boundary in the NR/IM blend.

The TEM observations corroborate the results obtained from the Kerner and van der Poel analysis for the blends that contain NR as the major component. Homogeneous, distinct inclusions are found in the micrographs, supporting the assumptions chosen in the calculations. The micrographs indicate that a wide distribution of inclusion size and shape exist in the structures of these blends. Moreover, the average size of inclusions in the NR/IM blend is larger than the average size of inclusions in the NR/BIIR blend. Nonetheless, self-consistent calculations were able to properly predict

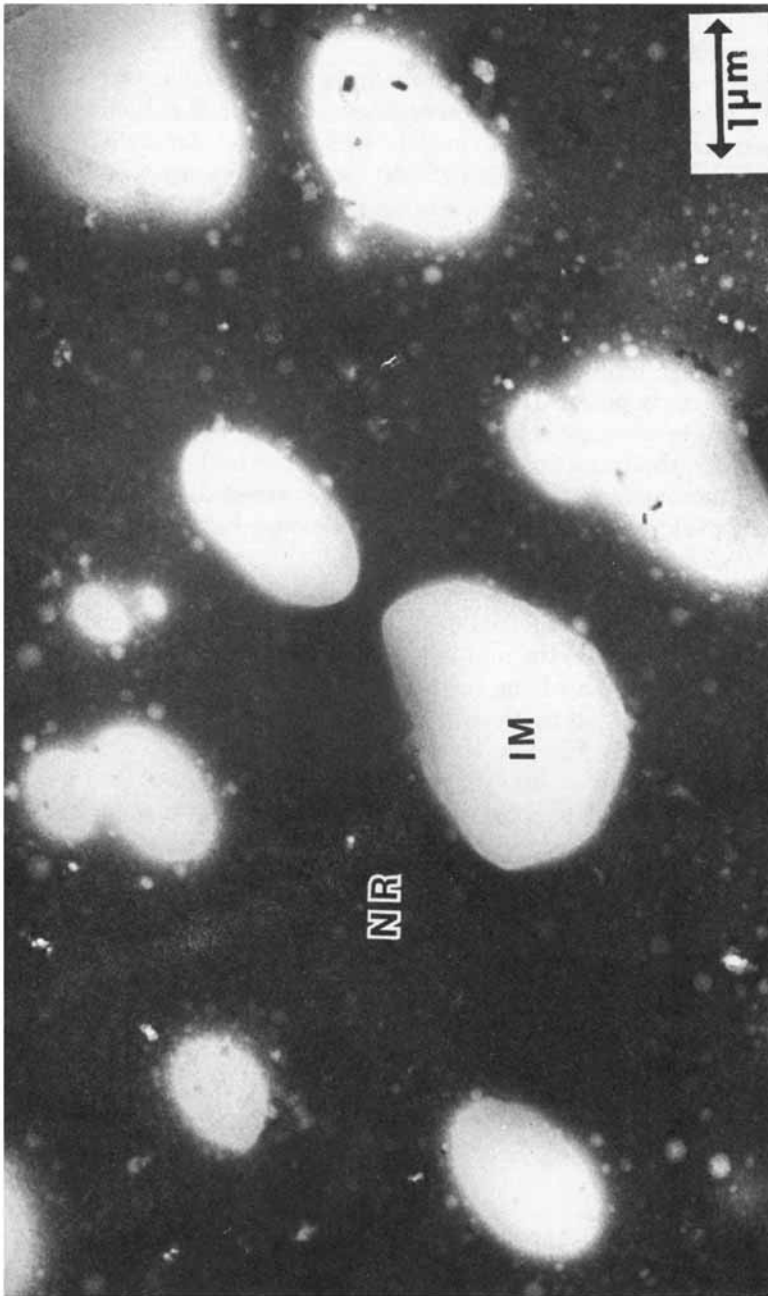


Fig. 3. Transmission electron micrograph of the stained NR/IM, 75/25 blend.

the mechanical behavior of both elastomer blends through the glass transition of the respective components.

Comparisons of theory and experiment for 50/50 blends of NR/BIIR and NR/IM were expected to be more severe tests of the theoretical models examined in this work. (The models were derived for spherical particles embedded in a matrix material.) For 50/50 blends, an a priori determination of the matrix (and included) phase is not possible. Experimental results for the 50/50 NR/BIIR blend are compared with the mean field calculations in Figure 4. The experimental data indicate that the height of the NR peak has been subdued relative to the 75/25 blend and the shoulder attributed to the transition of BIIR has heightened, in accordance with the composition change. The solid curve represents the Kerner calculation with the assumption that NR is the matrix phase. The dashed curve represents the van der Poel result with the same assumption. Neither theory is able to model the mechanical data through the transition region. We attempted both calculations assuming BIIR as the matrix phase. This assumption lowered the NR peak and raised the BIIR peak (as expected), but did not produce better agreement with the data.

The theoretical expressions explored in this work, derived for particulate-filled matrices, are not expected to accurately predict mechanical properties of 50/50 mixtures because the morphology of the 50/50 blends is not expected to match the description of the model structure used in their derivation. This conclusion is supported by electron micrographs of the 50/50 NR/BIIR blend shown in Figure 5. (Similar results were obtained for the 50/50 NR/IM blend.) Three regions of differing electron densities are identified in the figure. The heavily stained NR phase accounts for the darkest regions and the BIIR phase appears in the areas with medium density. The composition of the light regions could not be ascertained. Each phase appears continuous through the

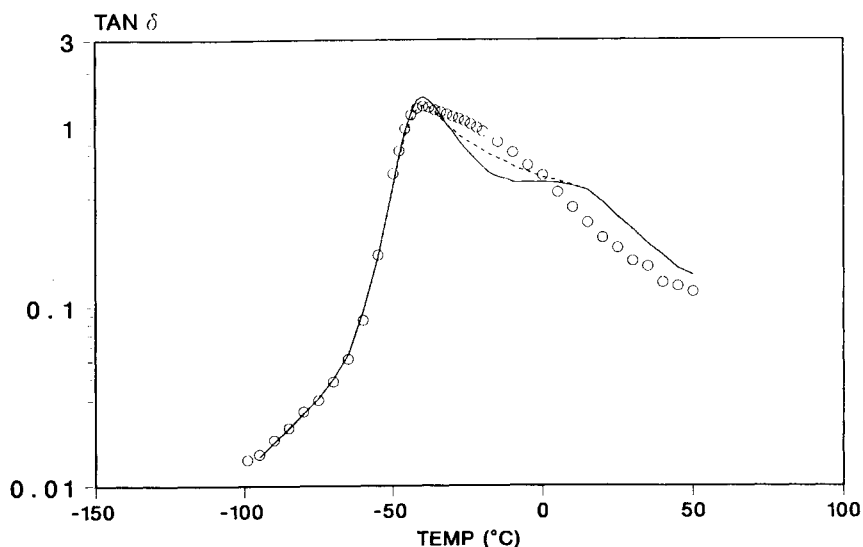


Fig. 4. Loss tangent vs. temperature for the NR/BIIR, 50/50 blend. Kerner calculations are represented by the solid line and van der Poel calculations are represented by the dashed line.

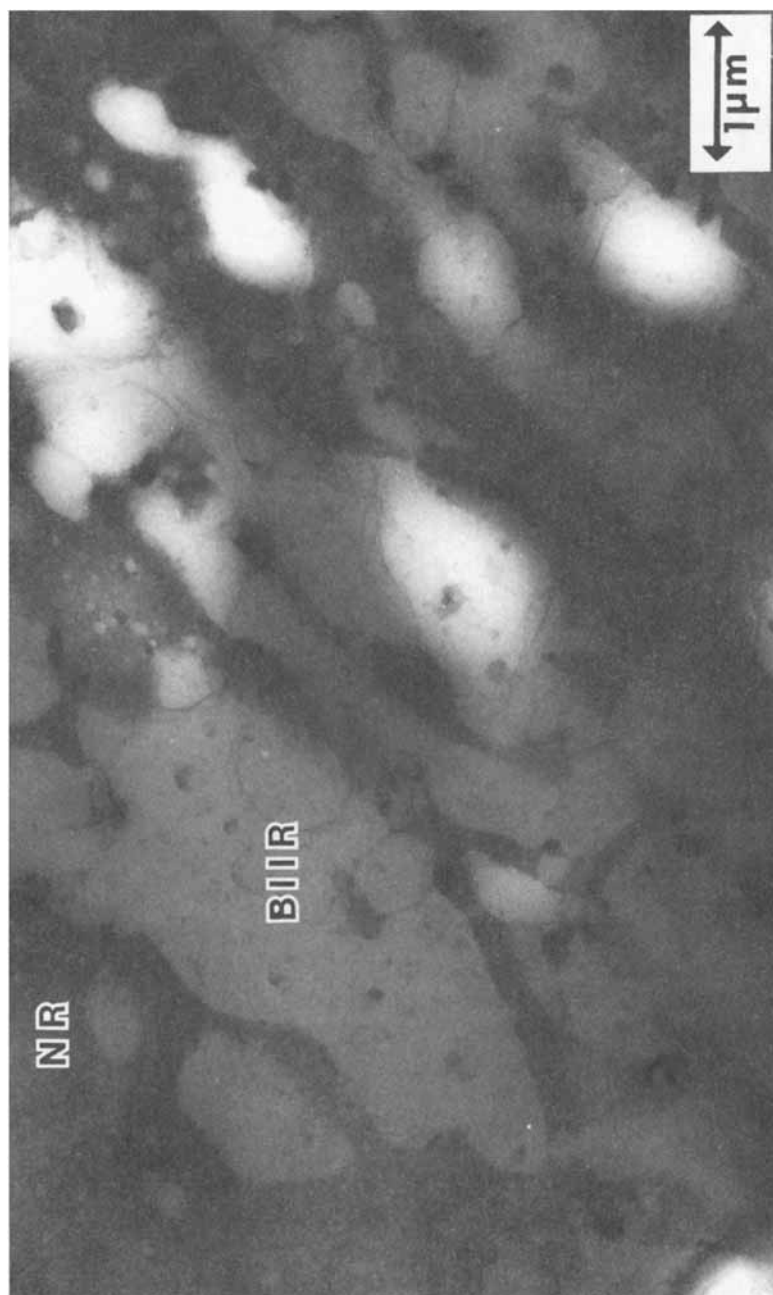


Fig. 5. Transmission electron micrograph of the stained NR/BIIIR, 50/50 blend.

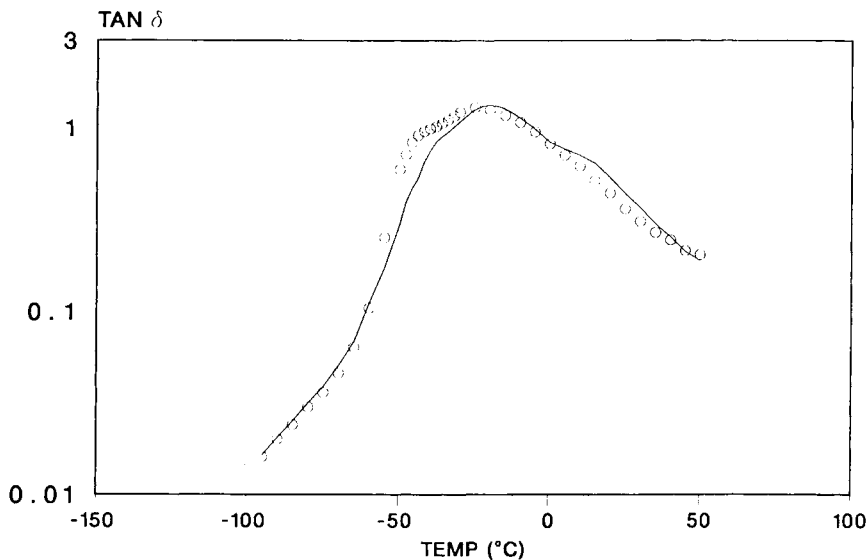


Fig. 6. Loss tangent vs. temperature for the NR/BIIR, 25/75 blend. Kerner and van der Poel calculations are represented by the solid line.

micrograph, in contrast to the model structure used in the development of the theoretical expressions.

A composition of a NR/BIIR blend was chosen to make BIIR the major component. (A corresponding NR/IM blend could not be prepared due to excessive bubble formation during molding.) Mechanical data and theoretical calculations assuming BIIR as the matrix phase are compared in Figure 6. Again, the volume fraction of inclusions (NR) used in the calculations was 0.25. And we assumed the inclusions were homogeneous. The good agreement between theory and experiment show that the Kerner and van der Poel/Smith equations are equally applicable to blends with BIIR as the major component.

The 25/75 NR/BIIR blend structure assumed in the calculation described above was verified with TEM. A micrograph of the 25/75 NR/BIIR blend (Fig. 7) depicts a morphology that is qualitatively consistent with the structure described for the Kerner and van der Poel model. Like the 75/25 NR/IM and 75/25 NR/BIIR blends, the dark included regions of NR are found in a light, BIIR matrix. But the NR inclusions are thin, discontinuous webs that differ from the generally spherical inclusions found in the 75/25 NR/BIIR and NR/IM blends. Apparently, the model calculations (at the experimental temperatures and frequency) are not sensitive to these details in the structure of the blend. Studies at different times (frequencies) and temperatures may show that the detail in structure will affect the accuracy of the Kerner and van der Poel equations in other regimes of molecular relaxation.

CONCLUSIONS

The Kerner and van der Poel/Smith equations were successfully applied to several elastomer blends over a range of temperature and time (frequency) that encompass the glass transition of the respective components. We have

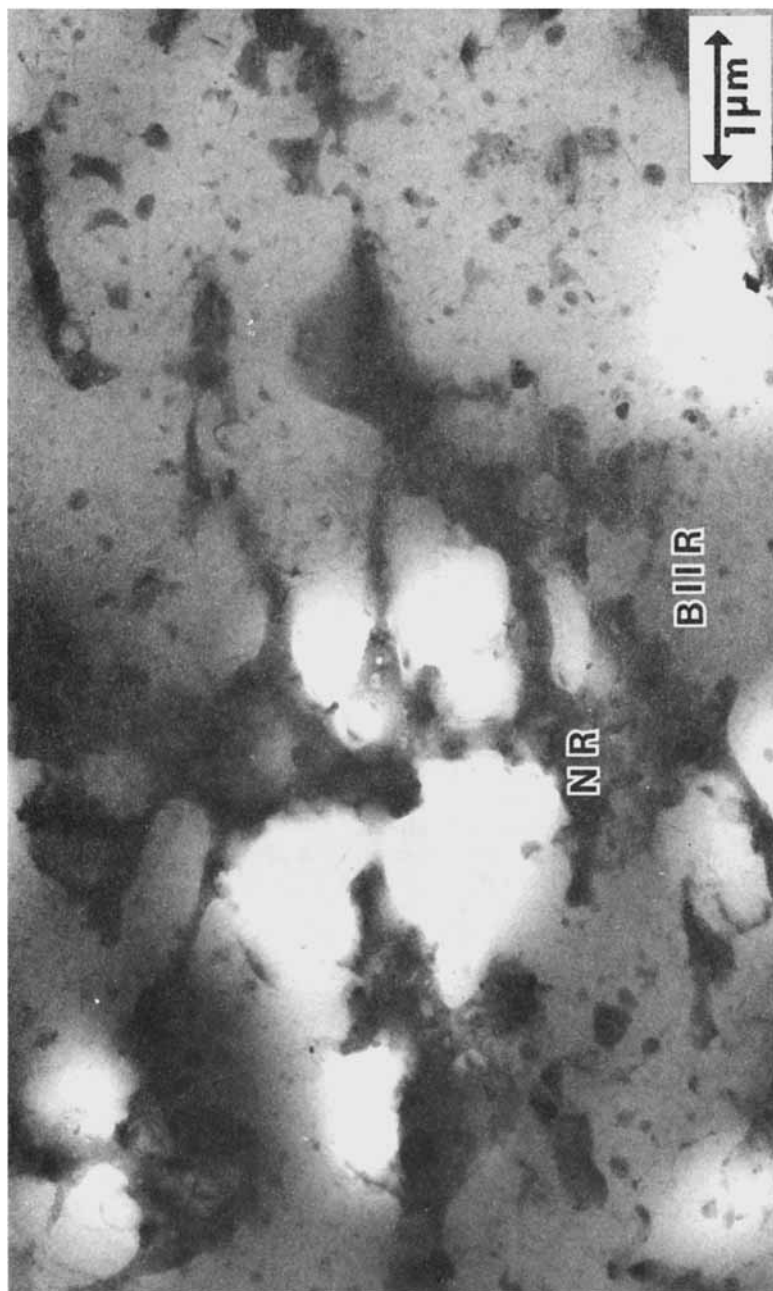


Fig. 7. Transmission electron micrograph of the stained NR/BIIIR, 25/75 blend.

found that the accuracy of these equations depends on the structure of the elastomer blend. In general, the theories were able to model experimental data for blends with well-defined inclusions in a matrix material. This description of blend morphology most nearly matches the model structure used to derive the theoretical expressions. Our results show that the detailed structure of the inclusions is not a controlling factor that determines the accuracy of the models. TEM analysis of 75/25 NR/BIIR and 25/75 NR/BIIR blends show that these materials exhibit a wide range of inclusion shape and size. The mechanical properties of each of these composites, however, were correctly predicted by both the Kerner and van der Poel/Smith equations.

In contrast, elastomer blends with structures that contain continuous regions of each phase (50/50 blends) are not accurately modeled by the Kerner and van der Poel/Smith theories. As expected, and verified by TEM, these structures do not correspond to the model used to derive the self-consistent expressions. For these structures, Kerner's "aggregate" model^{1,5} may prove useful for predicting mechanical data. We are currently working on the solution of this equation for the viscoelastic case and the application of these results to elastomer blends.

References

1. E. H. Kerner, *Proc. Phys. Soc.*, **69B**, 808 (1956).
2. C. van der Poel, *Rheol. Acta*, **1**, 198 (1958).
3. J. C. Smith, *J. Res. Nat. Bur. Std. U.S.*, **78A**, 355 (1974).
4. J. C. Smith, *J. Res. Nat. Bur. Std. U.S.*, **79A**, 419 (1975).
5. R. A. Dickie, in *Polymer Blends*, D. R. Paul and S. Newman, Ed., Academic Press, New York, 1978.
6. R. A. Dickie, *J. Appl. Polym. Sci.*, **17**, 79 (1973).
7. F. R. Schwarzl, H. W. Bree, C. G. Nederveen, G. A. Schwippert, L. C. E. Struik, and C. van der Wal, *Rheol. Acta*, **5**, 270 (1966).
8. R. A. Dickie, *J. Appl. Polym. Sci.*, **17**, 45 (1973).
9. K. A. Mazich, M. A. Samus, P. C. Killgoar, Jr., and H. K. Plummer, Jr., *Rubber Chem. Tech.*, **59**, 623 (1986).

Received February 9, 1988

Accepted April 9, 1988